Biochar from wood waste as additive for structural concrete

BIOCHAR FROM WOOD WASTE AS ADDITIVE FOR STRUCTURAL CONCRETE

Alice Sirico[a], Patrizia Bernardi[a*], Corrado Sciancalepore[a,c], Francesca Vecchi[a], Alessio Malcevschi[b], Beatrice Belletti[a], Daniel Milanese[a,c]

[a] Department of Engineering and Architecture, University of Parma, Parco Area delle Scienze, 181/A, 43124 Parma, Italy

[b] Department of Chemistry, Life Sciences and Environmental Sustainability, University of Parma, Parco Area delle Scienze, 11/A, 43124 Parma, Italy

[c] National Interuniversity Consortium of Materials Science and Technology (INSTM), via G. Giusti 9, 50121 Florence, Italy

*Corresponding author. Tel. +39 0521 905709; fax +39 0521 905924

E-mail address: patrizia.bernardi@unipr.it

ABSTRACT

The environmental impacts of cement and concrete industries are increasingly taken into consideration by regulatory agencies and new solutions must be found to turn into more sustainable productions. The use of waste materials as partial replacement of cement and/or aggregates or also as fillers into cement-based admixtures is a possible way to reduce the related negative impacts, such as carbon dioxide emissions and raw materials consumption. This work explores the possibility of using biochar, a carbon-rich and porous solid by-product resulting from thermochemical conversion of residual biomass under controlled conditions, as filler in concrete for structural use. The biochar used in this study derives from a commercial plant, which produces energy from pyro-gasification of woodchips. Biochar is at first chemically and morphologically characterized, then it is added as filler in concrete in different percentages, up to 10% by weight of cement. The effects of its introduction on fresh and hardened physical and mechanical properties of concrete, as well as on the internal matrix microstructure, are evaluated and compared to a reference concrete. Different curing conditions (wet and dry) and curing times (up to 365 days) are processed, also in order to evaluate biochar effect on concrete in terms of internal curing action and long-term behavior.

KEYWORDS

Waste, circular materials, biochar, filler, concrete, mechanical characterization, carbon sink, sustainability.

1. INTRODUCTION

By 2030, 60% of the world's population is expected to live in cities. Although cities occupy only 3% of the Earth's land, they use 60%-80% of the world's energy and are responsible for 70% of the world's carbon emissions. The 2030 Agenda for Sustainable Development strongly encourages all possible efforts towards more sustainable cities and industries, as well as towards consumption and product processes that can promote economic prosperity and good health while protecting our environment [1]. The cement and concrete sector lies at the foundation of modern and future cities and it is therefore at the heart of efforts to improve the sustainability and resilience of the urban environment, by sustaining the population growth through the realization of environmentally friendly buildings [2,3].

The first step to achieve this target is surely the adoption of more sustainable construction materials. In this regard, the research attention has been focusing on concrete, which, with a production of almost 20 billion cubic meters, is the most widespread construction material in the world. It is worth saying that, since 1990s cement and concrete producers have shown an increasing attention to the polluting emissions, the used energy and the consumption of natural resources connected with its production. It should be noted that cement industry contributes about 5–7% to global anthropogenic CO_2 emissions, including the CO_2 released in the clinker industrial process from the calcination of limestone, from the combustion of fuels in the kiln, as well from the power generation [4–6]. The consumption of natural resources is significant too, since the production of 1 ton of Portland cement requires, on average, 1.53 tons of raw materials (1.22 tons of limestone and 0.31 ton of clay) [7]. The aggregates needed for concrete admixtures also determine a consistent consumption of not-renewable resources, like water, gravel, sand or crushed rock.

By implementing circular economy principles, several attempts have been made to reduce these negative impacts through the development of "eco-friendly" concretes, which try to re-use the organic or inorganic waste largely produced by industry and society, representing another pressing issue to solve. During the last decades, different kinds of industrial waste or recycled materials have been inserted into cement-based products to partially replace aggregates (mainly plastics, glass, fly ash, slag, construction and demolition waste

[8–14]) or cement (such as fly ash, silica fume, ground granulated blasted furnace slag, ceramic and glass waste [15]), with different results in terms of material performance.

In this framework, the research of greener alternatives for concrete production has brought to the attention the use of biochar, which is a solid waste obtained as by-product from the thermochemical conversion of biomass to bioenergy under controlled conditions. More in details, according to the European Biochar Certificate guidelines [16], biochar is defined as a char produced by biomass pyrolysis, a process whereby organic substances are broken down at temperatures ranging from 350°C to 1000°C in a low-oxygen environment. So, the resulting material is typically characterized by low ratio of H/C and O/C (which is considered as indicator for the degree of chemical stability and carbonization grade) and by high specific surface areas, high pore volumes and good absorptive capacity [17]. For its ability to fix a large fraction of carbon as well as for its porous structure and water retention property, biochar is nowadays used for a wide range of applications, mainly in the agricultural field as soil amendment, to enhance soil fertility, improve plant growth and provide crop nutrition. Its properties and effectiveness, as carbon dioxide sequestration material, make biochar interesting to be used also inside construction materials, as a strategy not only for waste management, but also for storing carbon in a stable form in buildings. The first research attempts have been addressed to the use of biochar as filler or cement replacement into cement-based materials. Several experimental studies on cement pastes [18–22] and mortars [23–28] were carried out to verify biochar compatibility with the cementitious matrix and its effect on physical and mechanical properties, few of them considering also the effect of biochar addition on durability [29,30]. Since biochar is generally characterized by a low bulk density, low thermal conductivity and high porosity, lighter materials with increased thermal insulation and sound absorption properties can be produced [31]. Moreover, when inserted into cement-based materials, its porous microstructure promotes water retention in the mixing stage [27,32]. This determines an important loss in workability, which would require additional water in the mix with consequent decrease of mechanical strengths. Nonetheless, the use of superplasticizer can help to solve this problem by overcoming the adverse effect of the addition of biochar on flowability [27]. On the other hand, the absorbed water is released at a later stage, promoting secondary additional reaction and additional curing and so partially improving mechanical properties. The research of biochar as additive in cement pastes showed that small percentages (up to about 1% by cement weight) could improve mechanical properties, while higher quantities tend to result in a decrease

(also significant) of mechanical strength [18,19]. When used in cement mortars, good structural performances can be obtained with a slightly increased percentage (up to about 2.5÷5.0% by cement weight) [23–27]. More limited is the research developed on the use of biochar in concrete or in ultra-high performance concrete (UHPC), exploring both its function as cement replacement [33–36] or as additive [13,31,37] to modify concrete properties. However, its introduction into concrete mix is surely interesting, since higher percentages can generally be adopted, thus increasing the recycling rate. Anyway, results obtained from literature on cementitious materials are very scattered, since they are strongly influenced by the intrinsic characteristics of the used biochar, which in turn depend on several parameters: the type of initial biomass and its original pore size and ash content, the temperature of production, the type of conversion process and the residence time at elevated temperature. Biochar can be produced through slow pyrolysis (temperature range 400°C - 650°C), fast pyrolysis (650°C - 850°C), or gasification, which generally occurs between 900°C and 1100°C. The main product of these processes is syngas, with char and liquids (tar) as waste by-products. Most of the studies in technical literature regard the use of biochar derived from pyrolysis plants, which are often built on research purpose in a lab/pilot-scale, while research on chars derived from commercial plants is still scarce [38,39]. However, biochar produced by industrial pyro-gasification plants, which are generally intended for electric and thermal energy production, represents a significant volume of waste material to dispose of. Hence, research for an industrial implementation of the reuse of this waste into construction materials is still needed.

This work aims at studying the effect of the addition of a biochar derived from an industrial pyro-gasification power plant into a standard concrete recipe (cement, sand, coarse aggregate). After a chemical and morphological characterization of biochar, this is added as a filler in a reference concrete mix in different percentages, up to 10% by weight of cement, so to evaluate its effect on concrete in terms of workability, density, shrinkage, compressive and flexural strength, and post-cracking behavior. The fresh and hardened physical-mechanical properties of the developed “eco-concretes”, as well as their internal matrix microstructure, are evaluated and compared to a reference concrete without biochar. Different curing conditions (wet and dry) and curing times (up to 365 days) are processed. Since the development of the mechanical strength with time plays a major role for design practice, and research on biochar-added cement-based materials has not been focused on this aspect yet, this work also aims to provide some insights on the effects of biochar addition on long-term behavior of concrete.

2. MATERIALS AND METHODS

2.1 Cement and aggregates

Portland-limestone cement CEM II/A-LL 42.5 R (conforming to Standard EN 197-1 [40]) was used for all the concrete admixtures of the research program. This type of cement contains from 80 to 94% of Portland cement clinker and from 6 to 20% of limestone, with a total organic carbon (TOC) content not exceeding 0.2% by mass and average declared contents of Sulfate (SO_3) and Chloride (Cl) equal to 2.8 and 0.09%, respectively. Cement fineness is represented by a specific surface area through Blaine method of 3900 cm^2/g.

Locally available calcareous sand, with maximum particle size of 4 mm (81.8% passing the 2 mm sieve) and a siliceous stone, with maximum particle size of 10 mm (83.9% passing the 8 mm sieve), were used as aggregates. The corresponding grading curves are reported in Figure 1, for both fine and coarse aggregates. The water absorption, which is defined as the water content of an aggregate in the saturated surface dry (SSD) condition, was determined for both sand and gravel according to EN 1097-6 [41], obtaining values equal to 1.75% and 2%, respectively.

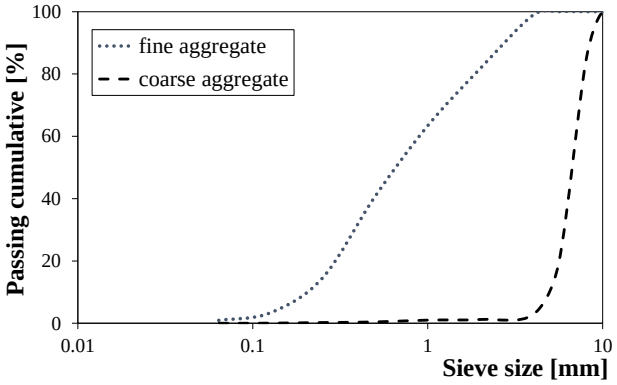

Figure 1 – Grading curves of fine and coarse aggregates.

2.2 Biochar

2.2.1 Production and collection

The biochar was collected from a biomass pyro-gasification power plant mainly intended for electricity and heat generation according to the principle of combined heat and power (CHP). This plant is located in the North of Italy and uses as feedstock wood waste from local forests (mainly broadleaf trees, such as chestnut, pine and fir), with an initial variable moisture content between 25÷40%, depending on the season. Woodchips with size between 30 mm and 90 mm (Fig. 2a) are first dried (T ≅ 75-80°C) to reduce moisture content under

8%, then transported from the storage bunker to the plant (Fig. 2b) by a screw conveyor. Tar-less wood gas is then produced from biomass in a controlled process based on the downdraft principle, i.e. the wood chips and the wood gas move in the same direction. Various oxidation chemical reactions take place in the plant (Fig. 2c) releasing the heat needed for the endothermic reactions, with the final production of syngas and carbon. Syngas is the result of reactions occurring between char and oxygen present in sub-stoichiometric amounts, to form a mix of carbon monoxide, carbon dioxide and water. The syngas is cooled in several steps and cleaned (Fig. 2d) then floats ashore a gas engine and generates electricity. The produced char, which has no immediate use and it is considered as a waste to dispose of, is discharged in an ash box and further transported outside the plant (Fig. 2e).

The biochar powder was characterized and used as received from the plant (Fig. 2f), without further treatments (like sieving or grinding), so allowing to reduce the environmental impacts and make the recycling process more sustainable. Several physical-chemical analyses were at first carried out to characterize biochar in terms of morphology, structure and composition, so to evaluate its use into cementitious materials.


(a)

(b)


(c)
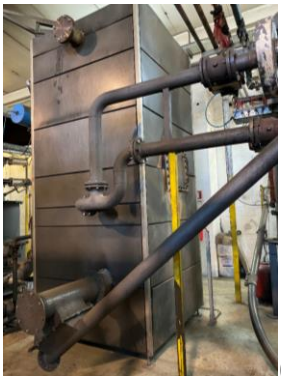
(d)

(e)

(f)

Figure 2 – (a) Input woodchip biomass; (b) drier; (c) gasifier; (d) component for syngas filtering and cooling; (e) biochar collection; (f) biochar used for the experimental campaign.

2.2.2 Particle size distribution, density and morphology

Biochar size distribution was analyzed with a laser granulometer (Mastersizer 3000, Malvern Instruments Ltd., Malvern, UK), using the Fraunhofer approximation. The particle size analysis was conducted in wet mode, employing water as dispersing medium. Volume density values in % were obtained as a function of the particle size in μm.

The solid density (also known as true or skeletal density) of biochar is calculated by the helium pycnometer Ultrapyc 1200e (Quantachrome Instruments, Boynton Beach, USA). About 4 grams of powder were placed in the small (10.8 cm^3) sample cell, and the density was expressed as the mean of 20 measurements. Helium-based solid density is a technique by which helium gas is used to access the open porosity in the solid sample and thereby measure the solid volume and any closed porosity.

The biochar bulk density is determined by measuring the weight of un-compacted volume of particles by means of an analytical balance and a known volume measuring cell. The expressed value is the mean of 5 different samples. Bulk (or apparent) density represents the density of a larger volume of biochar particles and includes the solid phases, the particle (open and closed) pores and the interparticle voids.

Scanning electron microscopy (SEM) characterizations were performed by means of a field emission SEM (FESEM, Nova NanoSEM 450, FEI company, USA). Images were acquired in field-free lens mode making use of the circular backscatter detector (CBS). The accelerating voltage (HV) of 15 kV, the spot size of 4 μm and the working distance (WD) of about 6 mm were utilized in the acquisition of all images. SEM analysis was performed both on biochar and biochar-added concrete samples.

2.2.3 Chemical properties and composition

Chemical elemental analysis was performed by means of the energy-dispersive X-ray spectroscopy system (X-EDS) QUANTAX-200 (Bruker, Germany), equipped with a silicon drift detector (SDD) XFlash 6/10.

Heavy metal content of solid biochar was determined via Inductively Coupled Plasma Mass Spectrometry (ICP-MS) according to EN 13657 + EN ISO 11885 [42,43] for the total concentration of Ni, Pb, K, Cu, Na, Zn and according to EPA 8270E [44] to determine PAHs concentration.

2.2.4 Chemical structure

X-ray diffraction (XRD - X'pert PRO, PANalytical, Almelo, Netherlands) on biochar sample was carried out in the 10-100° 2θ angular range by using the CuKα radiation ($\lambda K\alpha_1$ = 0.15406 nm, $\lambda K\alpha_2$ = 0.15444 nm); the scan was acquired with a step size of 0.05° 2θ and counting time of 30 s.

Biochar infrared (IR) spectrum was recorded on a Spectrum Two FT-IR spectrometer (Perkin Elmer, UK) in attenuated total reflectance (ATR) mode. The spectra were recorded between 4000 and 400 cm^{-1}, with a resolution of 4 cm^{-1} and 32 scans.

The pH was measured with a glass electrode (SevenCompact Duo, Mettler-Toledo, Columbus, OH, United States) in a 1:5 (v/v) biochar/deionized water mixture after 1h shaking and stabilization, according to ISO 10390 [45] and EN 13038 [46] respectively.

In order to estimate the degree of disorder in the biochar structure, Raman measurements were carried out using a micro-Raman system (Labram instrument Jobin Yvon-Horiba, Japan) at room temperature employing an excitation laser emitting at the wavelength of 532 nm with a total exposure time of 250 s.

2.2.5 Thermogravimetric analysis (TGA)

In the thermogravimetric analysis (TGA 8000, Perkin Elmer, UK) powder sample was heated from 20 to 800°C at a ramp of 10°C min^{-1} in N_2 atmosphere.

2.3 Biochar-added concrete

2.3.1 Mix design and workability tests

A reference plain concrete (PC) mix was first prepared, following a recommended recipe for standard applications. Aggregates were first oven dried, then they were properly combined by mixing 66.67% fine with 33.33% coarse fraction, so to obtain an aggregate grading curve as close as possible to classical Fuller and Bolomey ones. Water was added at a ratio of 0.5:1 to the cement, as reported in Table 1, together with the other proportions of the PC mix components, all expressed with respect to the cement amount. As can be read from Table 2, an acrylic based superplasticizer (Mapei Dynamon Xtend W202R) was also used to improve concrete workability, so to obtain a consistence class S4 (slump in the range 160-210 mm, as defined in EN 206-1 [47]) determined by slump test on fresh concrete (EN 12350-2 [48]). The mixing sequence was conceived so to obtain a homogeneous mixture: dry aggregates were first mixed with half of the required water

in a standard concrete mixing machine for 5 min, then the cement and a quarter of total water were added and mixed for about 3 min. Finally, superplasticizer and the remaining water were added for last 4 min mixing.

Mix	Cement	Fine aggregate	Coarse aggregate	Water
PC	1	2.75	1.375	0.5

Table 1 – Reference plain concrete (PC) mix proportions with respect to cement weight.

Subsequently, four biochar-added concrete admixtures were prepared, by adding biochar in increasing percentages from 2.5 to 10% (by weight of cement) to the reference PC mix. The mixing sequence was the same as PC: biochar was added in the very first stage, together with aggregates and half water, where biochar was pre-soaked for 48h up so to reach its saturation point. Table 2 reports the four resulting biochar-added concrete batches, each identified with letters BC followed by the corresponding biochar addition percentage. A significant color change from light to dark grey, produced by increasing biochar additions, was observed in concrete mixes, as clearly evidenced in Figure 4.

It is worth noticing that in all the produced admixtures, the same mix design as PC (Tab.1) was used, except for the superplasticizer dosage, which was accommodated to balance the loss in workability due to biochar addition. The required superplasticizer amount was determined so to obtain through slump test almost the same consistence level (class S4) for all the admixtures. Table 2 reports the superplasticizer percentages (by weight of cement) used for all the admixtures and the corresponding measured slump. As can be better appreciated from Figure 3, it was necessary to increase the superplasticizer dosage for increased biochar percentages to obtain the same workability, due to the water absorption in biochar pores.

Mix	Biochar [% by wt. of cement]	Superplasticizer [% by wt. of cement]	Slump (EN 12350-2) [mm]
PC	0	0.95	200
BC-2.5	2.5	1.25	190
BC-5.0	5.0	1.60	195
BC-7.5	7.5	2.50	175
BC-10.0	10	3.33	30

Table 2 – Plain and biochar-added concrete batches: superplasticizer amount and slump test results.

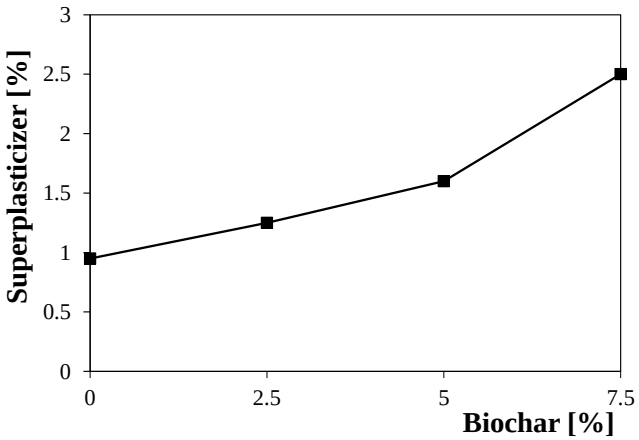

Figure 3 – Required superplasticizer amount (% by wt. of cement) for increasing biochar addition up to 7.5 % (by wt. of cement), to obtain the same slump class S4.

An addition of 10% biochar was tempted, but keeping constant the w/c ratio it was not possible to achieve a slump class different from S1 (slump in the range 10-40 mm, as defined in EN 206 [47]) with a reasonable amount of superplasticizer, so only a limited experimental characterization was performed on this last admixture.

2.3.2 Specimen preparation and curing conditions

Three different steel molds were used to produce samples for physical-mechanical tests (Fig. 4):

- cubes, 150 mm x 150 mm x 150 mm, for density measurements and compressive tests;
- cylinders, 100 mm diameter x 200 mm height, for splitting tests;
- prisms, 100 mm x 100 mm x 400 mm, for shrinkage and three-point bending tests.

Figure 4 – Cubical, cylindrical and prismatic specimens cast for the experimental campaign.

The molds were filled in two (prisms and cubes) or three (cylinders) layers, then concrete was compacted using internal vibrator to avoid segregation. The test specimens were left in the molds at room temperature, covered

with polyethylene sheets, for 1 day before being removed. To study the influence of curing conditions, above all on final strengths, two regimes were considered: wet curing (W) in water, and/or dry curing (D) at room temperature. Moreover, to investigate the influence of biochar addition on strength development, different curing times were scheduled: 7, 28 and 365 days. It is worth noticing that since the test schedule had to be modified due to the long shutdown related to Covid-2019 pandemic, some test specimens were cast twice to respect short-term curing times, producing additional samples for 100 days curing time.

Table 3 reports the number of specimens cast for each admixture to test under compression, tensile or bending, after different curing regimes (wet or dry) and times (7, 28, 100, 365 days).

For PC and BC-5.0 concrete mix, three additional prisms for shrinkage tests were cast, while for all the admixtures three cubes for density determination were prepared, so resulting in a total of 200 test specimens produced in the whole experimental campaign.

Curing time (days)	**7**	**28**			**100**			**365**		
Test	**C**	**C**	**SP**	**3PB**	**C**	**SP**	**3PB**	**C**	**SP**	**3PB**
PC	3W 3D	4W 3D	3W 3D	3W 3D	6W	6W	6W	3W 3D	3W 3D	3W 3D
BC-2.5	3W	3W 3D	3W 3D	3W 3D	-	-	-	-	-	-
BC-5.0	5W 3D	4W 3D	3W 3D	3W 3D	8W	6W	9W	3W 3D	3W 3D	3W 3D
BC-7.5	3W	3W 3D	3W 3D	3W 3D	-	-	-	-	-	-
BC-10.0	-	3W	5W	-	-	-	-	-	-	-

Table 3 – Overview of the mechanical tests (C= compressive, SP= tensile splitting, 3PB = three-point bending test) scheduled at different curing times (7-28-100-365 days): number of plain and biochar-added concrete specimens for testing after dry (D) or wet (W) curing conditions.

2.3.3 Density and shrinkage tests

Density of fresh concrete was obtained according to EN 12350-6 [49]. Moreover, density of hardened concrete was evaluated 28 days after demolding according to EN 12390-7 [50] by drying three cube specimens for each batch in a ventilated oven at 105±5 °C until the mass change in 24 h was less than 0.2%.

Free linear shrinkage was determined by measuring the change in length of specimen longitudinal axis by using two analogue dial indicators having 25 mm travel by 0.01 mm subdivision. The specimens were horizontally posed over several cylindrical supports to avoid frictions. The start of shrinkage measurements was at the age of 24 h up to the age of 60 days under dry curing condition.

2.3.4 Compressive tests

Compressive tests on 15 cm cube specimens were carried out following the procedure detailed in EN 12390-3 [51]. A Universal Testing Machine up to 3000 kN (METROCOM PV P30) was used to apply the load, with an accuracy of 1%. The load was increased continuously at a constant rate of 0.5 MPa/s until specimen failure.

2.3.5 Splitting and flexural tests

In order to evaluate the behavior in tension, splitting and flexural tests were performed in compliance with EN 12390-6 [52] and JCI-S-001 [53], respectively. This last Japanese Standard was chosen so to determine through the test not only the flexural strength, but also the associated fracture energy of the material.

To perform tensile splitting tests, cylindrical specimens with a length/diameter ratio equal to 2 were placed horizontally in the Testing Machine (METROCOM PV P30), between two parallel plane platens. A compressive force was applied along specimen length at a constant rate of 0.05MPa/s until no greater load could be sustained (Fig. 5).

Figure 5 – Splitting test execution and cracked specimen after failure.

Flexural tests were performed on notched beams under three-point loading (Fig. 6a-b). A central notch 2 mm wide and 30 mm deep (i.e. 0.3D, where D is the beam depth) was cut through a concrete saw the day of testing (Fig. 6a). The notched beams were placed over a net span of 300 mm (Fig. 6b) in a high-precision servo-electric Universal Testing Machine (INSTRON 8862) working under Crack Mouth Opening Displacement (CMOD) control, by using a clip-on gauge. A load cell fixed to the machine measured continuously the load.

This allowed providing for each specimen the total load - CMOD curve until failure and analyzing the material response in terms of both flexural strength σ_f and post-cracking residual behavior, through the evaluation of the fracture energy G_f. The initial loading (CMOD) rate was calibrated so to reach the peak load within 5 min from the start of the test. Over the peak load, the test speed was gradually increased until a residual load of about 0.02 kN was reached.

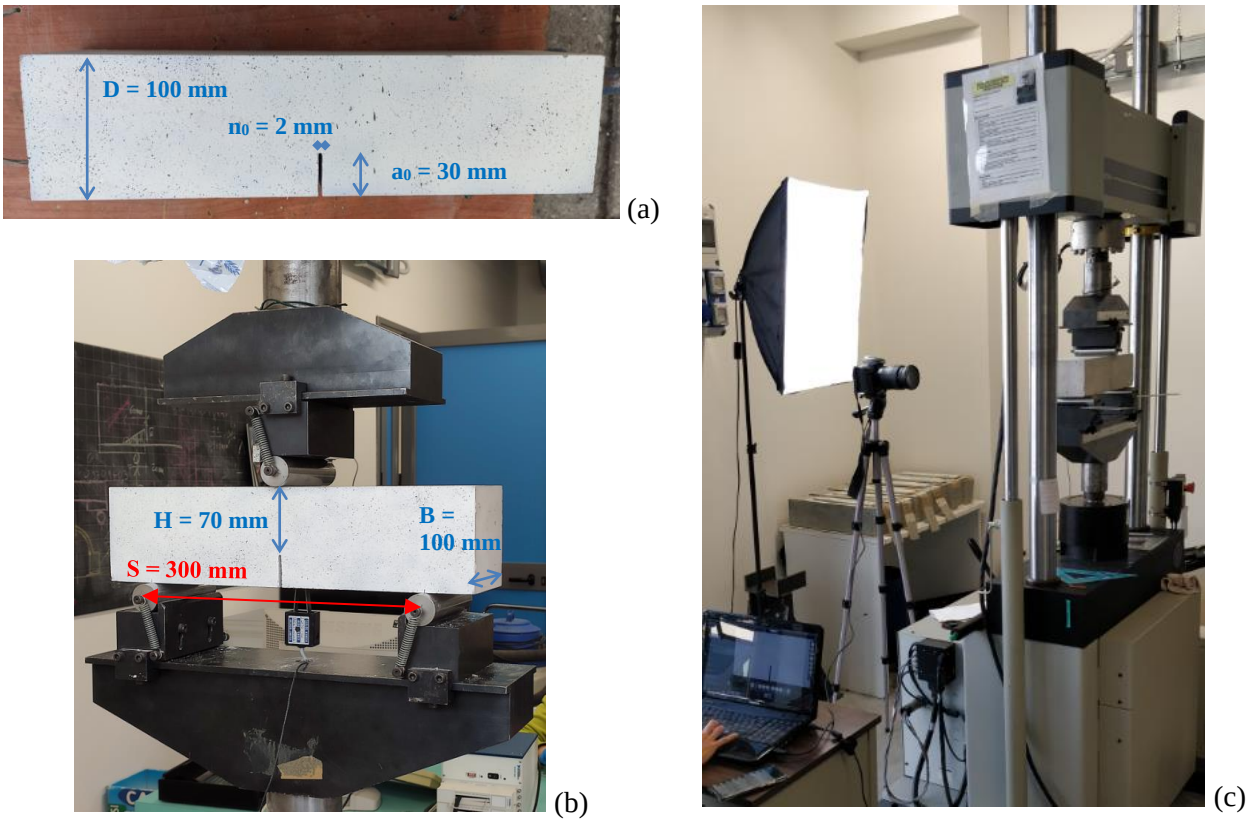

Figure 6 – (a) Prismatic specimen prepared for three-point bending test (3PBT) and DIC; (b) notched beam placed on the Universal Testing Machine: loading set-up with the clip-on gauge across the notch; (c) 3PBT and DIC set-up.

Digital Image Correlation (DIC) technique was also applied to obtain more information concerning the displacement field and crack pattern evolution during three-point bending tests. To this aim, before test, a random, high-contrast spackle pattern was produced on one lateral surface of each beam by first spraying a white paint and then making black dots with a paintbrush (Fig. 6a). The images were acquired using a digital camera NIKON D750 (24.3 Megapixel full frame), placed on a tripod perpendicularly to the specimen surface, under an adequate light source. The test set-up is shown in Fig. 6c. The open-source DIC software package

Ncorr implemented in MATLAB was used to elaborate the images and so to obtain the displacement and strain field generated during the test.

3. RESULTS AND DISCUSSION

3.1 Biochar characterization

Table 4 reports the main results obtained from the physical characterization of biochar particles. Biochar solid density depends on both feedstock and pyrolysis conditions [54]. For the biochar used in the experimental work, the solid density value resulted equal to 2.04±0.01 g/cm^3, a value in line with relatively high production temperatures and inorganic mineral content, as revealed by TGA analyses.

The dry bulk density value obtained was equal to 0.38±0.01 g/cm^3. Considering the starting wood, the given value falls in the linear relationship between the bulk densities of charcoals and their feedstock, as determined in [55].

The biochar particles distribution is relatively broad, with the standard percentiles of grain size D10, D50, D90 values respectively of 11.4, 107, 634 μm and the distribution width, i.e. the span, equal to 5.789. The volume weighted mean, $D_{V\text{-}mean}$ is found to be 236±60 μm. The results of biochar size analysis are compared to the equivalent analysis made on cement and on the sand used in the experimental campaign. As can be seen from Figure 7, biochar cumulative curve is intermediate between cement and sand, with maximum particle size lower than 3 mm.

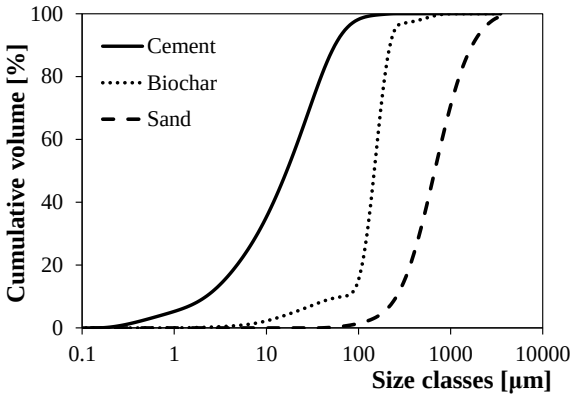

Figure 7 –Cumulative volume distribution of biochar particles compared to cement and sand grading curves.

% > 1 mm	%> 0.075 mm	D10 [mm]	D50 [mm]	D90 [mm]	True density [g/cm^3]	Bulk density [g/cm^3]
2.25	60	0.011	0.107	0.634	2.04±0.01	0.38±0.01

Table 4 – Biochar physical properties as determined by analysis of grain size and density.

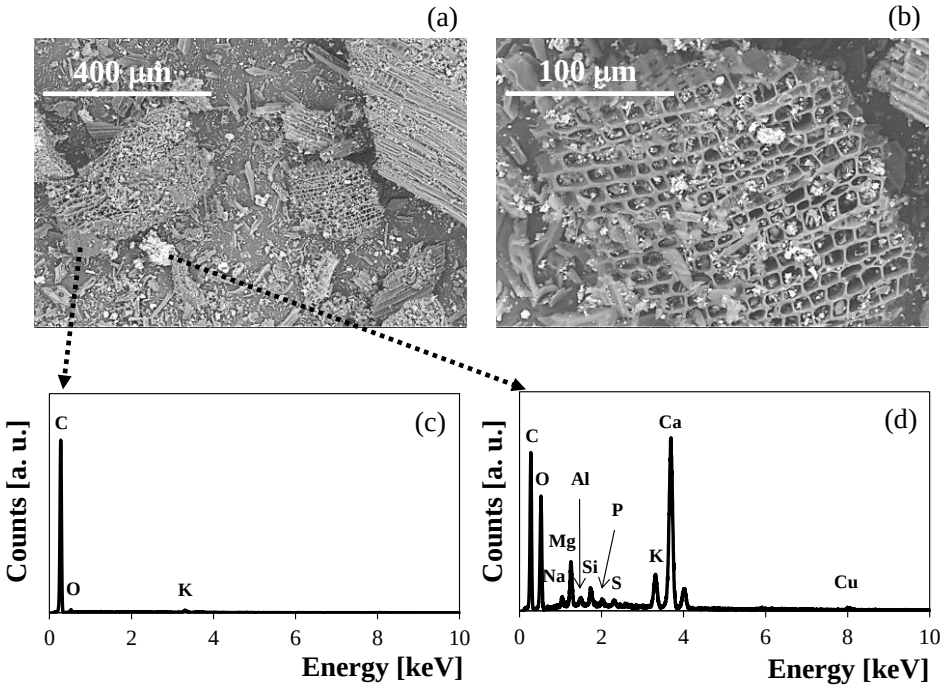

Figure 8 – SEM images of biochar particles at two different magnifications, (a) and (b), and EDS spectra of two particles with different composition, mainly carbonaceous (c) and heterogeneous (d), respectively.

The wide dimensional distribution of the biochar particles is confirmed by the SEM images, reported in Figure 8. The biochar particles show very heterogeneous dimensions, ranging from few microns to millimeter size (Fig. 8a). In the larger structures, it is possible to recognize the porous tubular organization typical of wood, from which the biochar was obtained (Fig. 8b). Furthermore, the SEM images, acquired by the signal deriving from the backscattered electrons, reveal the presence of particles with a higher image contrast and therefore with a different composition compared to the biochar carbon fragments.

The EDS spectra highlights the mainly carbonaceous composition of the darker particles, (Fig. 8c), while the brighter structures consist of substances based on alkaline and alkaline earth elements (Na, K, Ca and Mg) and other metallic and non-metallic elements such as Si, P, Al, S and Cu (Fig. 8d). However, in this case

considerable quantities of carbon and oxygen have been also detected, suggesting the presence of inorganic oxides and carbonates. In particular, the XRD analysis displays the presence of a prevalent crystalline phase, attributable to calcium carbonate ($CaCO_3$ - ICSD collection code 040107), (Fig. 9a). Moreover, in the diffraction spectrum at low 2θ values, a broad peak can be observed: this peak is attributable to the amorphous fraction of material present in the analyzed sample.

Tables 5 and 6 report the results of chemical analyses on biochar in terms of contents of heavy metals and polycyclic aromatic hydrocarbons (PAHs), respectively.

Element	**As**	**Cd**	**Cr**	**Ni**	**Pb**	**K**	**Cu**	**Na**	**Zn**
[mg/kg]	0.725	0.154	<10	24.2	<10	12.72	52.7	973	133

Table 5 – Heavy metal content (mg/kg) of biochar as obtained from ICP-MS.

PAH	**Value [mg/kg]**	**PAH**	**Value [mg/kg]**
Acenaphthene	0.05	Chrysene	<0.01
Acenaphthylene	0.02	Dibenz(a,h)anthracene	<0.01
Anthracene	0.02	Fluoranthene	<0.01
Benz(a)anthracene	0.03	Fluorene	0.22
Benzo(a)pyrene	<0.01	Indeno(1,2,3-c,d)pyrene	<0.01
Benzo(b)fluoranthene	0.05	Naphthalene	0.30
Benzo(k)fluoranthene	0.01	Phenanthrene	0.21
Benzo(g,h,i)perylene	<0.01	Pyrene	0.02

Table 6 – PAHs concentration [mg/kg] of biochar sample.

The presence of heavy metals and PAHs in biochar was evaluated as they represent a potential human and environmental health risk. Their concentration depends on the temperature of the production process and on their amount in the initial feedstock. Most heavy metals are more concentrated in the biochar than in the original biomass. However, biochar is able to effectively bind a number of heavy metals, thereby immobilizing them for a considerable long time. From Table 5, a considerable presence of Na e Zn and Cu can be observed, deriving not only from initial biomass but also from the mechanical pre-treatment of chipping [56]. In Table 6

the test results obtained for the 16 PAH priority compounds listed by US EPA [57] are reported. It can be noticed that their cumulative value is below the threshold established by International Guidelines (< 4 mg/kg for EBC [16]).

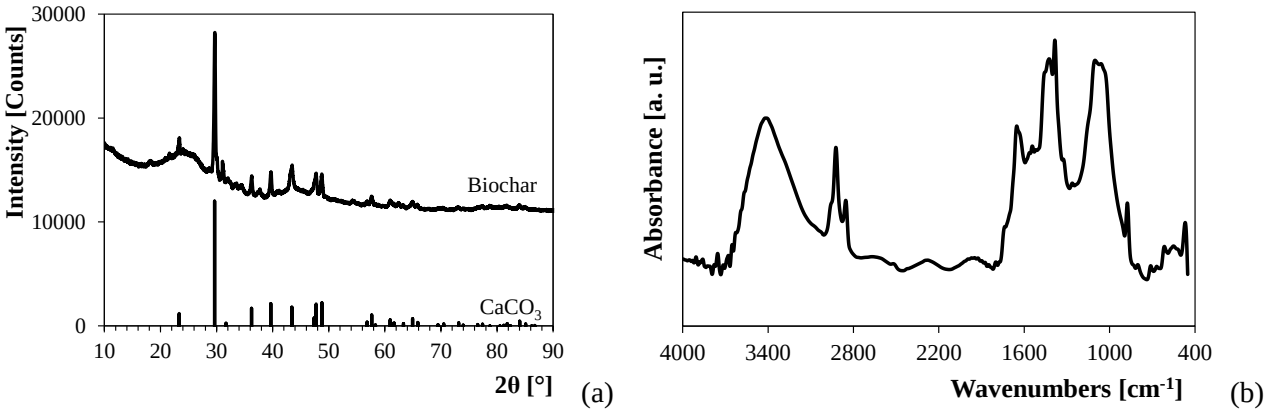

Figure 9 – (a) XRD spectrum of the biochar used for this study. Below the reference diffraction pattern of $CaCO_3$ is also reported; (b) IR spectrum of biochar sample.

The biochar IR spectrum allows to obtain information on the chemical structure, especially of the carbonaceous fraction (Fig. 9b). The broad band centered at 3400 cm^{-1} corresponds to the stretching vibrations of O-H groups, while the peaks at 2920 and 2850 cm^{-1} indicate an aliphatic C-H stretching vibration. The absorption peaks at about 1650, 1430 and 1080 cm^{-1} are designated respectively to C=C stretching, C-H bending and C-O stretching. The observed spectroscopic characteristics are consistent with those already described in literature [58,59].

Raman spectroscopy of biochar shows the typical spectrum of non-graphitic carbon materials with two main peaks: a narrower G peak (approximately 1590 cm^{-1}) attributed to in-plane vibrations of crystalline graphite, and a broader D peak (approximately 1350 cm^{-1}) attributed to disordered amorphous carbon (Fig. 10a) [60]. The Raman quality index (the I_D/I_G ratio ≈ 0.98, where I_D and I_G are respectively the heights of D and G peaks) highlights the enhanced graphitic structure of the used biochar [61].

The biochar pH value resulted equal to 11.46. Biochar is generally alkaline, and this is mainly related to the inorganic minerals such as carbonates and phosphates, and the ash formed during gasification and carbonization.

The quantitative evaluation of the inorganic component in the biochar can be carried out by the constant weight residue, obtained by the thermogravimetric curve (Fig. 10b). From a thermal point of view, biochar decomposes at around 500°C. Assuming the complete pyrolytic decomposition of the biochar carbonaceous portion, the residual inorganic component is about 19% of the initial weight of the sample. The biochar thermal degradation process can be divided into three steps. The first step is between room temperature and 100 °C, where a weight loss of about 6% represents the removal of the adsorbed water. The second step is in the range 450–550 °C, where a weight loss of about 50% indicates the main pyrolytic scission process of biochar carbonaceous portion. In the range 550–650 °C, a weight loss of about 6% is attributed to the final thermal decomposition of the more refractory residual organic components, such as the carbon skeleton structure [62].

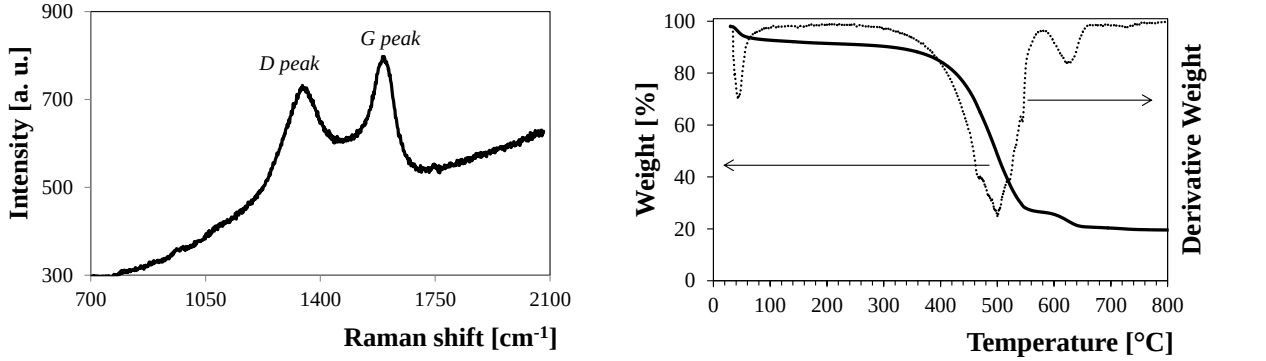

Figure 10 – (a) Raman spectrum of biochar sample; (b) TGA curve of biochar sample (on the left axis) and its derivate (on the right axis).

3.2 Biochar-added concrete

3.2.1 Optical and electronic microscopy

The dispersion and distribution of the biochar particles in the concrete matrix were evaluated by means of optical microscopy. The images in Figure 11 show a homogeneous dispersion, without the presence of aggregates or phase segregation.

The adhesion of biochar fillers to the concrete matrix is better evaluated by SEM characterization (Fig. 12). The SEM images show the biochar particles completely surrounded and wetted by the concrete matrix. No separation is noted at the interface between the external surface of the biochar and the concrete, indicating high compatibility and remarkable interaction between the hydration products of the cement matrix and the

hydrophilic functionalities (hydroxyl groups), detected by IR characterization, on the surface of biochar particles.

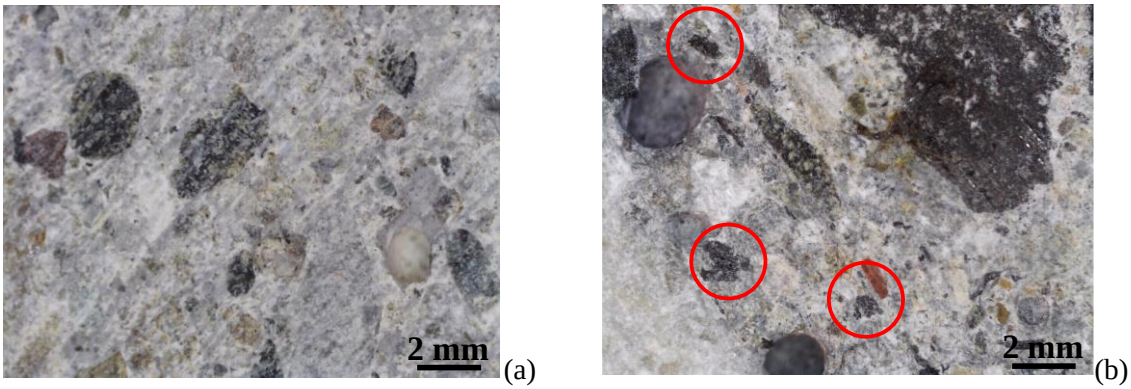

(a) (b)

Figure 11 – Optical micrographs of (a) unfilled concrete and (b) concrete added with 7.5% biochar as representative sample (the red circles indicate the biochar particles).

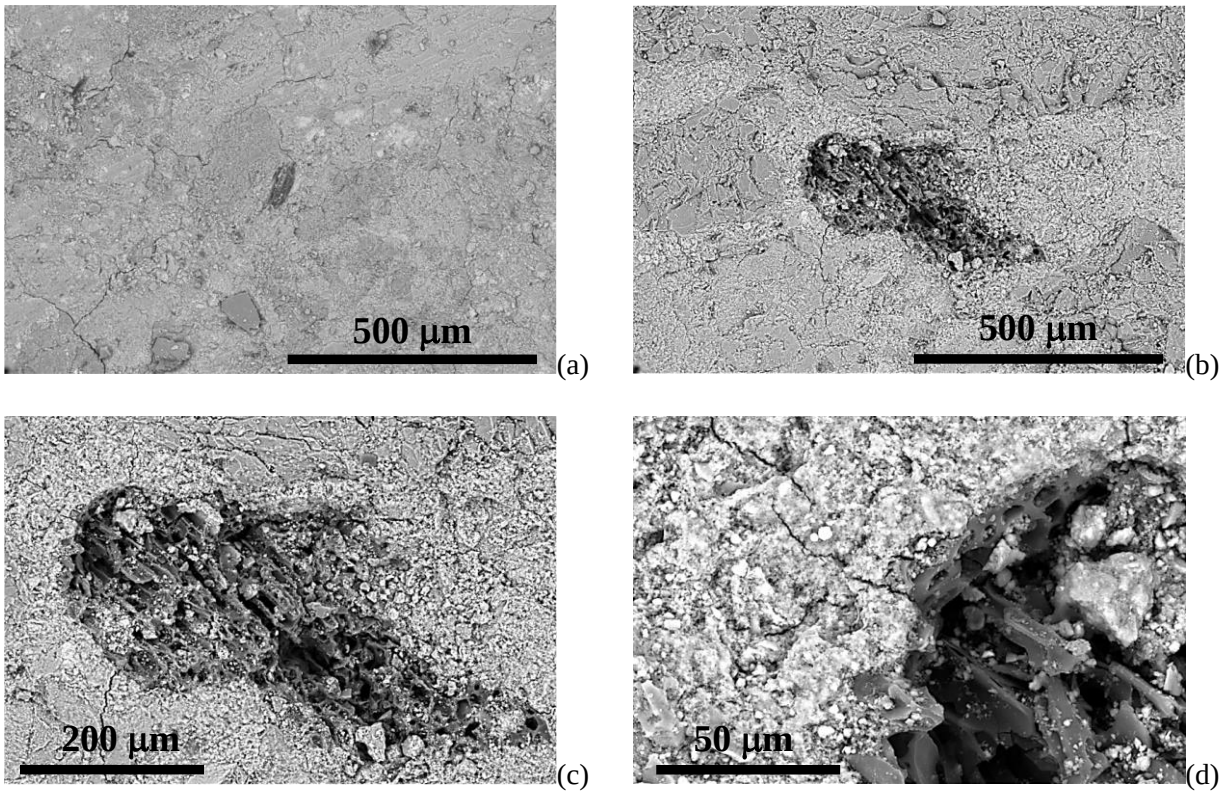

(a) (b) (c) (d)

Figure 12 – SEM images of (a) unfilled concrete and (b-d) a biochar particle in the concrete matrix at different magnifications.

3.2.2 Density and shrinkage

Fresh and hardened density values of concrete with different biochar additions are reported in Table 7. By comparing the values obtained with those of the reference plain concrete mix (PC), it can be observed that biochar has a limited influence on material density. The maximum density reduction obtained for hardened concrete specimens with 10% biochar addition is about 5% with respect to PC density value, so it can be concluded that biochar has not a significant effect on the final weight.

The same can be said for the impact of biochar on shrinkage (Fig. 13). The strain measurements, registered up to 60 days from casting, were almost the same for plain concrete and 5% biochar-added concrete specimens.

Mix	Fresh Density kg/m^3	Hardened density kg/m^3
PC	2291	2119
BC-2.5	2265	2117
BC-5.0	2275	2078
BC-7.5	2261	2040
BC-10.0	2245	2013

Table 7 – Fresh and hardened density of plain and biochar-added concrete batches.

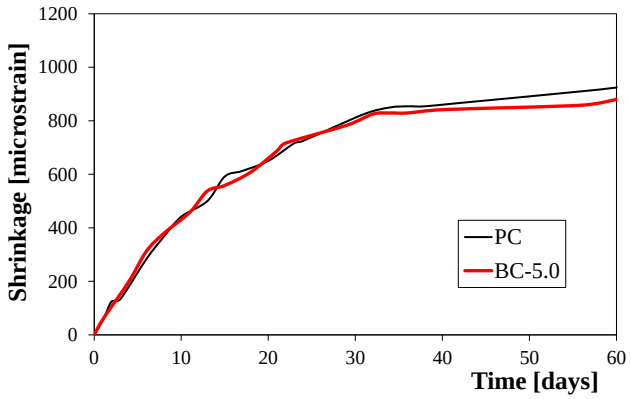

Figure 13 – Development of shrinkage strain with time for plain and 5% biochar-added concrete.

3.2.3 Compressive strength

The effect of biochar addition on compressive strength is more remarkable, as can be observed from Figure 14a-b, which reports the compressive strength average values and standard deviations obtained for the several

considered curing times and conditions. By considering 28-days strength, it can be stated that additions up to 5% of biochar are not only possible, but also able to determine a slight increase in compressive strength, which become more evident for dry curing of specimens. In case of dry conditions, the improvement of compressive strength for concrete with the addition of 5% of biochar respect to control are indeed statistically robust for all the curing times considered, as confirm by the one-factor variance analysis (ANOVA) performed. The ANOVA study employs a level of significance of 5%, which implies a 95% probability of biochar effect being significant. On the contrary, higher biochar additions result in a negative impact on strength, more significant after water curing (with a decrease of 19% and 33% with respect to plain concrete for 7.5% and 10% biochar addition, respectively, Fig. 14a). This fact, also considering the loss in workability already highlighted in previous section 2.3.1, makes biochar additions higher than 5% not recommended in structural concrete. To compare the results obtained from water and dry curing, it is worth noticing that the beneficial effect of biochar on strength development is more noticeable in case of dry curing, for both short and long curing times. The water restrained in biochar pores is gradually released with time, and this promotes the development of hydration reactions as also highlighted in [33]. By comparing the average values of 28-days compressive strengths, the strength increment with respect to plain concrete in case of water curing is around 5% and 3%, for 2.5% and 5% biochar addition respectively (Fig. 14a). Such increases exceed 25% and 17% for dry curing (Fig. 14b). Focusing the attention on 5% biochar-added concrete, a significant increase with respect to plain concrete can be seen also at both 7 and 365 days of curing. Moreover, for this same batch, the positive effect of biochar as internal curing agent can be also recognized, since the development of strength from 28 to 365 days is higher for biochar-added concrete compared to the reference one. This can be better appreciated in Figure 15, where the development of concrete compressive strength in water or dry curing condition from 7 to 365 days of plain concrete is compared to that obtained from 5% biochar-added specimens. In case of dry curing, no significant increase in strength occurs from 28 to 365 days for plain concrete (equal to about 2%), while biochar-added specimens show an increase of about 12%. A similar trend is observed also for water curing: in this case, the plain concrete specimens show a compressive strength increase after 365 days equal to 25%, but not as much as biochar specimens, which have an increase of about 34%.

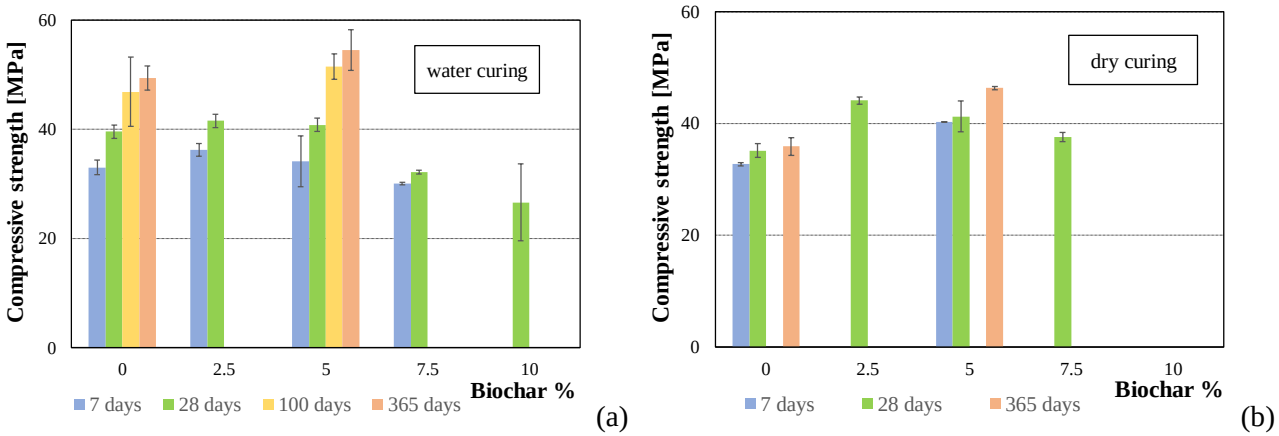

Figure 14 – Average compressive strength (and corresponding standard deviation) for different curing times (7 - 28 - 100 - 365 days) and conditions (water (a) and dry (b)) with increasing biochar additions (0 - 2.5 - 5 - 7.5 - 10 % by wt. of cement).

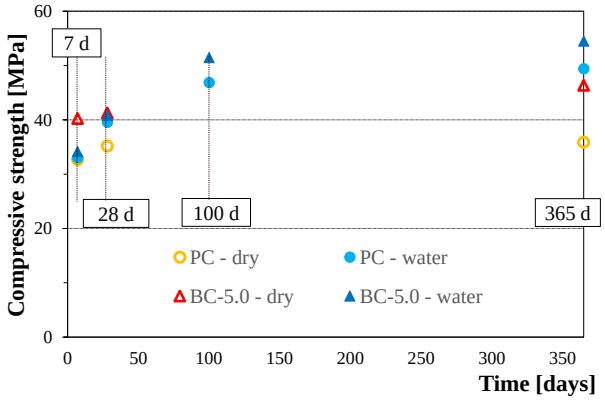

Figure 15 – Influence of 5% biochar addition on the development of concrete compressive strength in water or dry curing condition, from 7 to 365 days of curing time.

3.2.4 Tensile splitting and flexural strength

The addition of smaller percentages of biochar also improves the tensile behavior of concrete, which was investigated through splitting tensile and three-point bending (3PB) tests.

As can be seen from Figure 16a-b, the results of splitting test confirm that biochar additions up to 5% determine a strength increase with respect to plain concrete after 28 days of curing, for both water and dry conditions. On the contrary, higher additions determine a strength decrease in case of water curing, while a beneficial effect of biochar is confirmed for dry conditions.

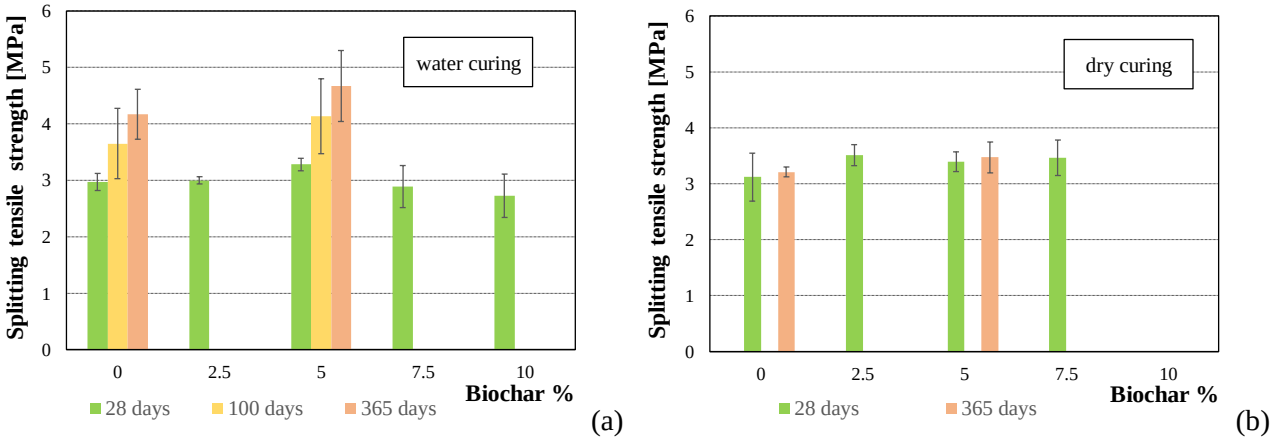

Figure 16 – Average splitting tensile strength (and corresponding standard deviation) for different curing times (28 - 100 - 365 days) and conditions (water (a) and dry (b)) with increasing biochar addition (0 - 2.5 - 5 - 7.5 - 10 % by wt. of cement).

Anyway, tension appears generally less affected than compression by strength variation with increasing biochar additions, as confirmed by the ANOVA analysis. This latter underlines indeed that there is not a statistically significant variation in splitting tensile strength when biochar is added to the admixtures. This effect is probably related to the formation of air voids in the tensile plane as a consequence of biochar particles addition, so resulting that the presence of biochar in the empty pores is less determinant to tensile strength, as already observed for mortars in [23]. Also in case of long-term behavior, the increase in strength of 5% biochar-added concrete specimens, from 28 to 365 days with water curing, was around 42%, comparable to the increase obtained for plain concrete ones (40%).

3PB tests under crack mouth opening displacement (CMOD) control allowed to obtain the full material response before and after cracking formation (see Figure 17, for all the batches at 28 days curing time and Figure 18, for plain and 5% biochar-added concrete at 365 days curing time). By comparing the obtained load P-CMOD responses, it can be generally stated that biochar has not a significant influence in the post-cracking response and consequently in the toughness of the material. Indeed, by comparing the fracture energy associated to each specimen (evaluated according to [53], where it is related to the area under the load P-CMOD curve), only small variations were registered from one batch to the other. The beneficial effect of biochar on fracture energy is known for mortars and, even more, for cement pastes [18,24]. However, the not significant improvement in fracture energy found in this study is not in contrast with the findings in literature,

since the toughening mechanisms of biochar particles that induce deviations in the crack path are obviously much more relevant for cement-based materials with no (or only fine) aggregates in their admixture. On the contrary, for concrete, the presence of coarse aggregates that provide themselves bridging and interlock actions across crack surfaces strongly mitigates the beneficial effects that biochar particles can offer.

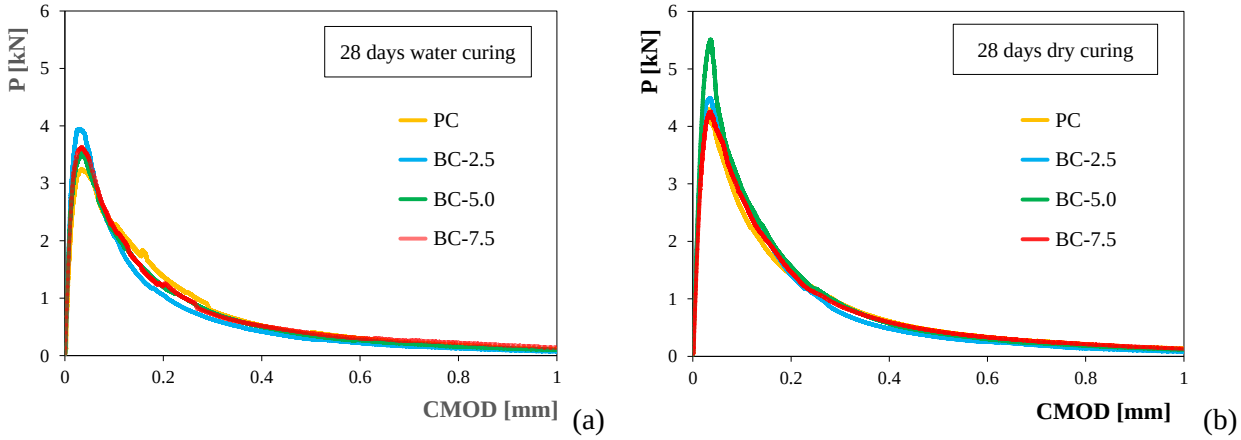

Figure 17 – Average load vs. CMOD response after 28 days (a) water or (b) dry curing, for concrete prismatic samples with increasing biochar addition (0 - 2.5 - 5 - 7.5 % by wt. of cement) under three-point bending test.

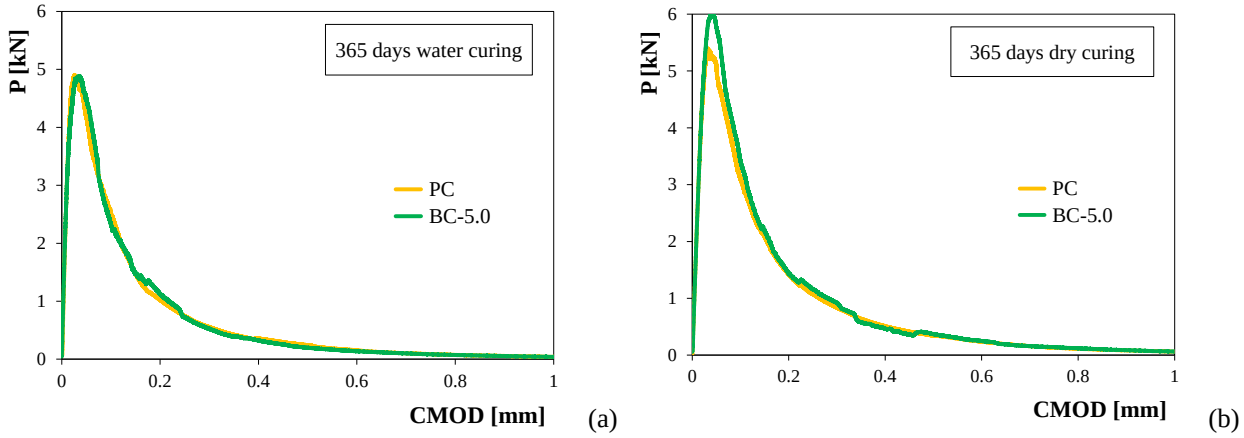

Figure 18 – Average load vs. CMOD response after 365 days (a) water or (b) dry curing, for concrete prismatic samples with increasing biochar addition (0 - 2.5 - 5 - 7.5 % by wt. of cement) under three-point bending test.

More significant are instead the differences in terms of average peak load P_{max} reached from each batch, from which the flexural strength $f_{ct,fl}$ was determined, according to the formula for notched beams, as $f_{ct,fl} = P_{max} \cdot (3S)/(2BH^2)$, where S, B and H are the beam span, width and net depth, respectively, as reported in Figure 6a-b. The average flexural strength values of each batch, reported in Figure 19 for different curing conditions and times, are indeed statistically different in case of 28 days of curing, even if the significance is

lower than in case of compression. In case of 28 days, for both water and dry curing, all the biochar-added concretes showed an increase of flexural strength with respect to plain concrete, with the best performance obtained by the 2.5% biochar addition in case of water and 5% biochar in case of dry curing (with an increase of about 27% and 29% with respect to plain concrete, respectively). As regards the strength development from 28 to 365 days, no significant differences were observed between plain and biochar-added concrete.

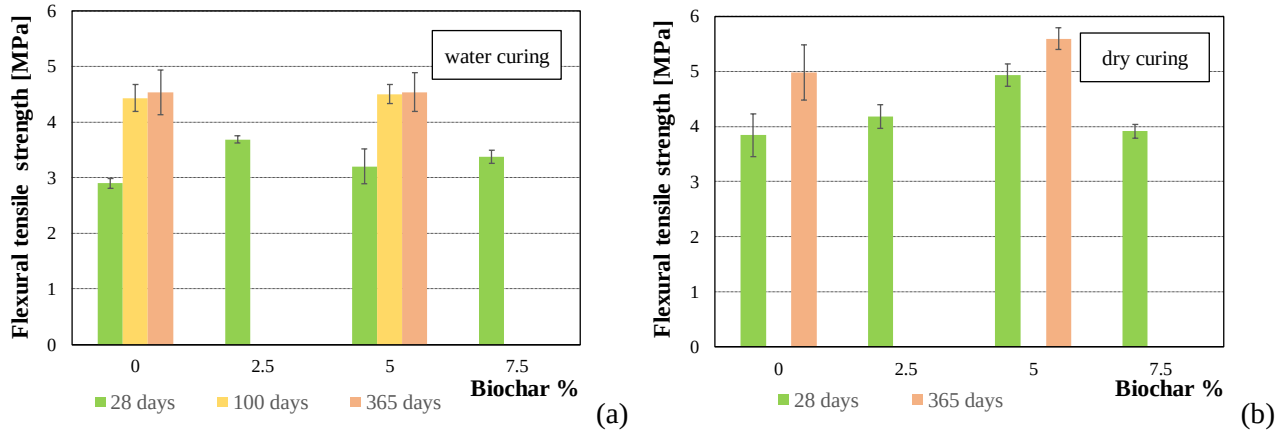

Figure 19 – Average flexural tensile strength (and corresponding standard deviation) by means of three-point bending test for different curing times (28 - 100 - 365 days) and conditions (water (a) and dry (b)) with increasing biochar addition (0 - 2.5 - 5 - 7.5 % by wt. of cement).

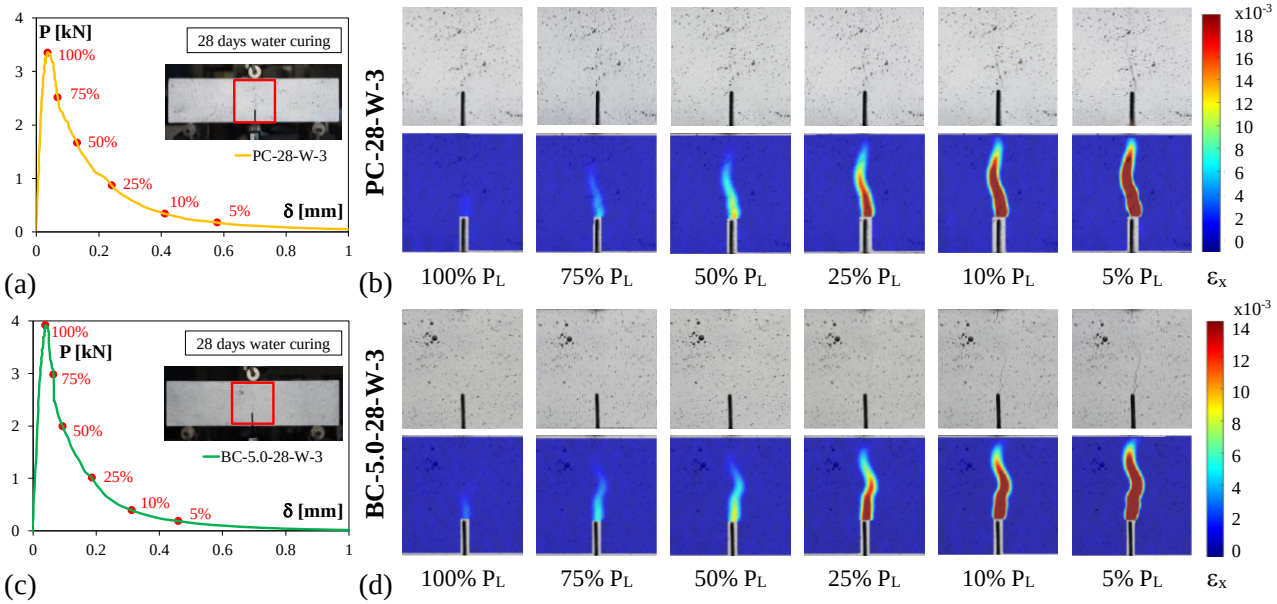

Figure 20 – Vertical displacement δ and horizontal strain ε_x field from DIC, elaborated in terms of Load P vs. midspan displacement δ curve (a, c) and in terms of crack pattern evolution near the notch (b, d) at 100%, 75%, 50%, 25%, 10%, 5% of Peak Load (P_L), for (a, b) plain concrete (PC) and (c, d) 5% biochar (BC-5.0) specimen number 3 tested after 28 days of water curing.

Lastly, during three-point bending tests, DIC technique was used to record the specimen strain and displacement field as well as the crack pattern development. Figure 20 reports, as an example, the load P vs. vertical midspan displacement δ curve and the crack pattern evolution near the notch in the post-cracking stage (until the 5% of peak load is reached) as obtained by DIC data elaboration, for a plain concrete (Fig. 20a-b) and for a 5% biochar-added (Fig. 20c-d) specimen after 28 days of water curing. The crack pattern development around the notch is almost the same for the two specimens as the CMOD increases and it can be concluded that the effect of biochar particles on crack propagation is negligible.

4. CONCLUSIONS

This work explored the effects of the incorporation of biochar particles, resulting from industrial pyro-gasification processes of wooden biomass, into standard concrete admixtures. The main results of the experimental investigation can be summarized as follows:

- Biochar particles show a very good compatibility with the cement matrix. No interphase separation between biochar and concrete occurs, as detected by SEM analyses.
- Workability is strongly affected by biochar addition. As the biochar addition increases, the same consistence of plain concrete can be only obtained or by increasing the superplasticizer dosage, if the same W/C ratio must be maintained, or otherwise by increasing the water content in the admixture. In the experimentation, to compare the results between the several batches, the W/C ratio was kept constant and equal to 0.5 and the maximum mixable biochar addition percentage resulted 7.5%, since 10% biochar addition determined too high superplasticizer amounts. An increased water addition was herein not attempted since this surely would have determined a decrease in mechanical strength.
- Concrete mechanical properties can be positively influenced by biochar additions. At 28 days of curing, the increase of compressive strength for 2.5% and 5% biochar addition resulted equal respectively to 5% and 3% for water curing and to 25% and 17% for dry curing. The percentage of 5% can then be considered as the optimal one, since even if the strength increment is slightly less, the potential recycling rate is higher. Biochar additions of 7.5% and 10% resulted in a strength decrease with respect to plain concrete respectively equal to 19% and 33% in case of water curing; consequently, additions in concrete greater than 5% are not advisable. Tensile behavior seems to be generally less affected by biochar additions in

terms of both splitting strength and cracking behavior. This latter is indeed not significantly influenced by biochar particles addition, as confirmed by DIC data. On the contrary, a significant improvement can be obtained in terms of flexural strength. Anyhow, by analyzing the overall tensile behavior of the tested specimens, the biochar percentage of 5% is confirmed to be the optimal one.

- As regard long-term behavior, the effect of biochar on strength development is more noticeable in compression and in particular the positive biochar impact is more evident when dry curing conditions are applied. The best improvement is obtained for 365 days of dry curing, which provides for 5% biochar addition an increase of almost 30% with respect to the reference plain concrete. The water restrained in biochar pores is gradually released with time, and this promotes hydration reactions and strength development. In case of dry curing conditions, while plain concrete does not show a significant strength increase from 28 to 365 days (only 2%), 5% biochar-added concrete shows on average an increase in compressive strength equal to 12%. The possibility of using biochar as internal curing agent, in particular in presence of dry curing conditions, which are very common in real building manufacturing, seems to be promising.
- The use into structural concrete of biochar from industrial pyro-gasification plants, which convert wooden biomass into electrical and thermal energy, represents a novelty with respect to technical literature and it is promising if the optimal percentage addition is first verified. The use of this waste allows the development of a circular construction material, also able to fix carbon in a stable form in buildings. The study can be extended to other biochar, produced by different plants and different feedstocks, and to other cementitious materials, in order to detect the best use of this by-product regarding the improvement of desired physical and mechanical performances.

ACKNOLEDGMENTS

This work was financially supported by Emilia Romagna Region in the framework of 2014/20 POR-FESR project “IMPReSA-betonplast: Development of innovative construction materials including non-recyclable plastic particles acting as reinforcement”, grant number PG/2018/632099. Authors gratefully acknowledge Mapei SpA for the precious advices in the mix design formulation, as well as Cementirossi SpA and Pizzarotti & C. SpA for providing raw materials for specimen preparation.

REFERENCES

[1] A.L. Salvia, W. Leal Filho, L.L. Brandli, J.S. Griebeler, Assessing research trends related to Sustainable Development Goals: local and global issues, J. Clean. Prod. 208 (2019) 841–849. doi:10.1016/j.jclepro.2018.09.242.

[2] M.A.B. Omer, T. Noguchi, A conceptual framework for understanding the contribution of building materials in the achievement of Sustainable Development Goals (SDGs), Sustain. Cities Soc. 52 (2020) 101869. doi:10.1016/j.scs.2019.101869.

[3] F. Johnsson, I. Karlsson, J. Rootzén, A. Ahlbäck, M. Gustavsson, The framing of a sustainable development goals assessment in decarbonizing the construction industry – Avoiding "Greenwashing," Renew. Sustain. Energy Rev. 131 (2020). doi:10.1016/j.rser.2020.110029.

[4] E. Worrell, L. Price, N. Martin, C. Hendriks, L.O. Meida, Carbon dioxide emissions from the global cement industry, Annu. Rev. Energy Environ. 26 (2001) 303–329.

[5] D.A. Salas, A.D. Ramirez, C.R. Rodríguez, D.M. Petroche, A.J. Boero, J. Duque-Rivera, Environmental impacts, life cycle assessment and potential improvement measures for cement production: A literature review, J. Clean. Prod. 113 (2016) 114–122. doi:10.1016/j.jclepro.2015.11.078.

[6] R. Maddalena, J.J. Roberts, A. Hamilton, Can Portland cement be replaced by low-carbon alternative materials? A study on the thermal properties and carbon emissions of innovative cements, J. Clean. Prod. 186 (2018) 933–942. doi:10.1016/j.jclepro.2018.02.138.

[7] L. Coppola, D. Coffetti, E. Crotti, G. Gazzaniga, T. Pastore, An Empathetic Added Sustainability Index (EASI) for cementitious based construction materials, J. Clean. Prod. 220 (2019) 475–482. doi:10.1016/j.jclepro.2019.02.160.

[8] M. Sandanayake, Y. Bouras, R. Haigh, Z. Vrcelj, Current sustainable trends of using waste materials in concrete—a decade review, Sustain. 12 (2020) 1–38. doi:10.3390/su12229622.

[9] N. Saikia, J. De Brito, Use of plastic waste as aggregate in cement mortar and concrete preparation: A

review, Constr. Build. Mater. 34 (2012) 385–401. doi:10.1016/j.conbuildmat.2012.02.066.

[10] C. Shi, K. Zheng, A review on the use of waste glasses in the production of cement and concrete, Resour. Conserv. Recycl. 52 (2007) 234–247. doi:10.1016/j.resconrec.2007.01.013.

[11] C. Shi, C. Meyer, A. Behnood, Utilization of copper slag in cement and concrete, Resour. Conserv. Recycl. 52 (2008) 1115–1120. doi:10.1016/j.resconrec.2008.06.008.

[12] V.W.Y. Tam, M. Soomro, A.C.J. Evangelista, A review of recycled aggregate in concrete applications (2000–2017), Constr. Build. Mater. 172 (2018) 272–292. doi:10.1016/j.conbuildmat.2018.03.240.

[13] A. Sirico, F. Vecchi, C. Sciancalepore, B. Belletti, P. Bernardi, A. Malcevschi, D. Milanese, Mechanical Properties of Concretes Containing Biochar and Recycled Plastic Aggregate, in: Fib Symp. "Concrete Struct. New Trends Eco-Efficiency Perform., 2021.

[14] E.E. Anike, M. Saidani, A.O. Olubanwo, M. Tyrer, E. Ganjian, Effect of mix design methods on the mechanical properties of steel fibre-reinforced concrete prepared with recycled aggregates from precast waste, Structures. 27 (2020) 664–672. doi:10.1016/j.istruc.2020.05.038.

[15] C.O. Nwankwo, G.O. Bamigboye, I.E.E. Davies, T.A. Michaels, High volume Portland cement replacement: A review, Constr. Build. Mater. 260 (2020). doi:10.1016/j.conbuildmat.2020.120445.

[16] European Biochar Foundation - European Biochar Certificate (EBC), Guidelines for a Sustainable Production of Biochar, Eur. Biochar Found. (2012) 1–22. doi:10.13140/RG.2.1.4658.7043.

[17] A. Tomczyk, Z. Sokołowska, P. Boguta, Biochar physicochemical properties: pyrolysis temperature and feedstock kind effects, Rev. Environ. Sci. Biotechnol. 19 (2020) 191–215. doi:10.1007/s11157-020-09523-3.

[18] L. Restuccia, G.A. Ferro, Promising low cost carbon-based materials to improve strength and toughness in cement composites, Constr. Build. Mater. 126 (2016) 1034–1043. doi:10.1016/j.conbuildmat.2016.09.101.

[19] A. Sirico, P. Bernardi, B. Belletti, A. Malcevschi, L. Restuccia, G.A. Ferro, D. Suarez-Riera, Biochar-based cement pastes and mortars with enhanced mechanical properties, Frat. Ed Integrita Strutt. 14 (2020) 297–316. doi:10.3221/IGF-ESIS.54.21.

[20] R.A. Khushnood, S. Ahmad, L. Restuccia, C. Spoto, P. Jagdale, J.M. Tulliani, G.A. Ferro, Carbonized nano/microparticles for enhanced mechanical properties and electromagnetic interference shielding of cementitious materials, Front. Struct. Civ. Eng. 10 (2016) 209–213. doi:10.1007/s11709-016-0330-5.

[21] R.A. Khushnood, S. Ahmad, P. Savi, J.M. Tulliani, M. Giorcelli, G.A. Ferro, Improvement in electromagnetic interference shielding effectiveness of cement composites using carbonaceous nano/micro inerts, Constr. Build. Mater. 85 (2015) 208–216. doi:10.1016/j.conbuildmat.2015.03.069.

[22] S. Ahmad, R.A. Khushnood, P. Jagdale, J.M. Tulliani, G.A. Ferro, High performance self-consolidating cementitious composites by using micro carbonized bamboo particles, Mater. Des. 76 (2015) 223–229. doi:10.1016/j.matdes.2015.03.048.

[23] S. Gupta, H.W. Kua, S.D. Pang, Biochar-mortar composite: Manufacturing, evaluation of physical properties and economic viability, Constr. Build. Mater. 167 (2018) 874–889. doi:10.1016/j.conbuildmat.2018.02.104.

[24] S. Gupta, H.W. Kua, H.J. Koh, Application of biochar from food and wood waste as green admixture for cement mortar, Sci. Total Environ. 619–620 (2018) 419–435. doi:10.1016/j.scitotenv.2017.11.044.

[25] S. Gupta, H.W. Kua, C.Y. Low, Use of biochar as carbon sequestering additive in cement mortar, Cem. Concr. Compos. 87 (2018) 110–129. doi:10.1016/j.cemconcomp.2017.12.009.

[26] S. Gupta, H.W. Kua, Carbonaceous micro-filler for cement: Effect of particle size and dosage of biochar on fresh and hardened properties of cement mortar, Sci. Total Environ. 662 (2019) 952–962. doi:10.1016/j.scitotenv.2019.01.269.

[27] A. Sirico, P. Bernardi, B. Belletti, A. Malcevschi, E. Dalcanale, I. Domenichelli, P. Fornoni, E.

Moretti, Mechanical characterization of cement-based materials containing biochar from gasification, Constr. Build. Mater. 246 (2020) 118490. doi:10.1016/j.conbuildmat.2020.118490.

[28] S. Gupta, H.W. Kua, S.D. Pang, Healing cement mortar by immobilization of bacteria in biochar: An integrated approach of self-healing and carbon sequestration, Cem. Concr. Compos. 86 (2018) 238–254. doi:10.1016/j.cemconcomp.2017.11.015.

[29] S. Gupta, A. Kashani, A.H. Mahmood, T. Han, Carbon sequestration in cementitious composites using biochar and fly ash – Effect on mechanical and durability properties, Constr. Build. Mater. 291 (2021) 123363. doi:10.1016/j.conbuildmat.2021.123363.

[30] S. Gupta, S. Muthukrishnan, H.W. Kua, Comparing influence of inert biochar and silica rich biochar on cement mortar – Hydration kinetics and durability under chloride and sulfate environment, Constr. Build. Mater. 268 (2021) 121142. doi:10.1016/j.conbuildmat.2020.121142.

[31] D. Cuthbertson, U. Berardi, C. Briens, F. Berruti, Biochar from residual biomass as a concrete filler for improved thermal and acoustic properties, Biomass and Bioenergy. 120 (2019) 77–83. doi:10.1016/j.biombioe.2018.11.007.

[32] S. Gupta, H.W. Kua, Effect of water entrainment by pre-soaked biochar particles on strength and permeability of cement mortar, Constr. Build. Mater. 159 (2018) 107–125. doi:10.1016/j.conbuildmat.2017.10.095.

[33] A. Dixit, S. Gupta, S.D. Pang, H.W. Kua, Waste Valorisation using biochar for cement replacement and internal curing in ultra-high performance concrete, J. Clean. Prod. 238 (2019). doi:10.1016/j.jclepro.2019.117876.

[34] A. Akhtar, A.K. Sarmah, Novel biochar-concrete composites: Manufacturing, characterization and evaluation of the mechanical properties, Sci. Total Environ. 616–617 (2018) 408–416. doi:10.1016/j.scitotenv.2017.10.319.

[35] Z. Asadi Zeidabadi, S. Bakhtiari, H. Abbaslou, A.R. Ghanizadeh, Synthesis, characterization and evaluation of biochar from agricultural waste biomass for use in building materials, Constr. Build.

Mater. 181 (2018) 301–308. doi:10.1016/j.conbuildmat.2018.05.271.

[36] S. Gupta, H.W. Kua, S.D. Pang, Effect of biochar on mechanical and permeability properties of concrete exposed to elevated temperature, Constr. Build. Mater. 234 (2020). doi:10.1016/j.conbuildmat.2019.117338.

[37] A. Dixit, A. Verma, S.D. Pang, Dual waste utilization in ultra-high performance concrete using biochar and marine clay, Cem. Concr. Compos. 120 (2021) 104049. doi:10.1016/j.cemconcomp.2021.104049.

[38] S. Meyer, B. Glaser, P. Quicker, Technical, economical, and climate-related aspects of biochar production technologies: A literature review, Environ. Sci. Technol. 45 (2011) 9473–9483. doi:10.1021/es201792c.

[39] V. Benedetti, F. Patuzzi, M. Baratieri, Characterization of char from biomass gasification and its similarities with activated carbon in adsorption applications, Appl. Energy. 227 (2018) 92–99. doi:10.1016/j.apenergy.2017.08.076.

[40] EN 197-1:2011, Cement – Part 1: Composition, specifications and conformity criteria for common cements, (2011).

[41] EN 1097-6:2013. Tests for mechanical and physical properties of aggregates - Part 6: Determination of particle density and water absorption, 2013.

[42] EN 13657:2002, Characterization of waste - Digestion for subsequent determination of aqua regia soluble portion of elements, (2002).

[43] EN ISO 11885:2009, Water quality - Determination of selected elements by inductively coupled plasma optical emission spectrometry (ICP-OES), (2009).

[44] U.S.EPA., Method 8270E (SW-846): Semivolatile Organic Compounds by Gas Chromatography/ Mass Spectrometry (GC/MS), 2018.

[45] ISO 10390:2021, Soil quality — Determination of pH, (2021).

[46] EN 13038:2011, Soil improvers and growing media - Determination of electrical conductivity, (2011).

[47] EN 206:2013, Concrete - Specification, performance, production and conformity, (2013).

[48] EN 12350-2:2019, Testing fresh concrete - Part 2: Slump test, (2019).

[49] EN 12350-6:2019, Testing fresh concrete - Part 6: Density, (2019).

[50] EN 12390-7:2019, Testing hardened concrete - Part 7: Density of hardened concrete, (2019).

[51] EN 12390-3:2019. Testing hardened concrete - Part 3: Compressive strength of test specimens, 2019.

[52] EN 12390-6:2009, Testing hardened concrete - Part 6: Tensile splitting strength of test specimens, (2009).

[53] JCI-S-001-2003. Method of test for fracture energy of concrete by use of notched beam, (2003).

[54] J.S. Pandolfo, A. G.; Amini-Amoli, M.; Killingley, Activated carbons prepared from shells of different coconut varieties, Carbon N. Y. 32 (1994) 1015–1019.

[55] C.E. Byrne, D.C. Nagle, Carbonized wood monoliths characterization, Carbon N. Y. 35 (1997) 267–273. doi:10.1016/S0008-6223(96)00135-2.

[56] F. Patuzzi, D. Basso, S. Vakalis, D. Antolini, S. Piazzi, V. Benedetti, E. Cordioli, M. Baratieri, State-of-the-art of small-scale biomass gasification systems: An extensive and unique monitoring review, Energy. 223 (2021). doi:10.1016/j.energy.2021.120039.

[57] US Environmental Protection Agency, Clean Water Act Priority Pollutants, (2013).

[58] H. Wang, C. Fang, Q. Wang, Y. Chu, Y. Song, Y. Chen, X. Xue, Sorption of tetracycline on biochar derived from rice straw and swine manure, RSC Adv. 8 (2018) 16260–16268. doi:10.1039/c8ra01454j.

[59] M. Keiluweit, P.S. Nico, M. Johnson, M. Kleber, Dynamic molecular structure of plant biomass-derived black carbon (biochar), Environ. Sci. Technol. 44 (2010) 1247–1253.

doi:10.1021/es9031419.

[60] M.M. Titirici, M. Antonietti, N. Baccile, Hydrothermal carbon from biomass: A comparison of the local structure from poly- to monosaccharides and pentoses/hexoses, Green Chem. 10 (2008) 1204–1212. doi:10.1039/b807009a.

[61] F. Tomul, Y. Arslan, B. Kabak, D. Trak, E. Kendüzler, E.C. Lima, H.N. Tran, Peanut shells-derived biochars prepared from different carbonization processes: Comparison of characterization and mechanism of naproxen adsorption in water, Sci. Total Environ. 726 (2020). doi:10.1016/j.scitotenv.2020.137828.

[62] P. Kim, A. Johnson, C.W. Edmunds, M. Radosevich, F. Vogt, T.G. Rials, N. Labbé, Surface functionality and carbon structures in lignocellulosic-derived biochars produced by fast pyrolysis, Energy and Fuels. 25 (2011) 4693–4703. doi:10.1021/ef200915s.